Original Article

Charge-reversible and biodegradable chitosan-based microgels for lysozyme-triggered release of vancomycin

Xin Li [a,b,c], Laura Hetjens [b], Nadja Wolter [b], Helin Li [a,*], Xiangyang Shi [d,e,*], Andrij Pich [b,c,f,*]

[a] Collaborative Innovation Center of Yangtze River Delta Region Green Pharmaceuticals, Zhejiang University of Technology, Hangzhou 310014, China
[b] DWI-Leibniz-Institute for Interactive Materials e.V, 52056 Aachen, Germany
[c] Institute of Technical and Macromolecular Chemistry, RWTH Aachen University, 52074 Aachen, Germany
[d] College of Chemistry, Chemical Engineering and Biotechnology, Donghua University, Shanghai 201620, China
[e] CQM-Centro de Química da Madeira, Universidade da Madeira, Campus da Penteada, 9000-390 Funchal, Portugal
[f] Aachen Maastricht Institute for Biobased Materials, Maastricht University, 6167 RD Geleen, the Netherlands

HIGHLIGHTS

- CH-PANI MGs with strong NIR absorption, pH-responsiveness, polyampholyte behavior and biodegradability are synthesized.
- Charge-reversal MGs are created by mild treatment with NaCl solution, and display high loading efficiency of cationic VM.
- The MGs exhibit excellent resistance to gastric acidity and prevent premature VM leakage in healthy intestinal tract.
- Lysozyme-triggered VM release renders the smart MGs with an obvious antibacterial activity.
- The smart MGs can be employed as potential oral delivery system for IBD treatment.

GRAPHICAL ABSTRACT
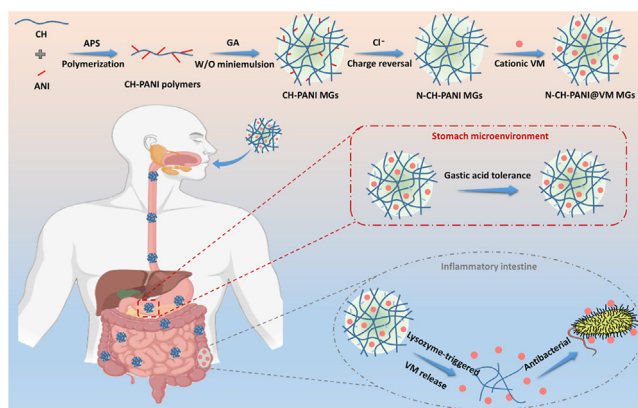
ABSTRACT

Introduction: High-dose drug administration for the conventional treatment of inflammatory bowel disease induces cumulative toxicity and serious side effects. Currently, few reports have introduced smart carriers for intestinal inflammation targeting toward the treatment of inflammatory bowel disease.
Objectives: For the unique lysozyme secretory microenvironment of the inflamed intestine, vancomycin-loaded chitosan-polyaniline microgels (CH-PANI MGs) were constructed for lysozyme-triggered VM release.
Methods: Aniline was first grafted to chitosan to form polymers that were crosslinked by glutaraldehyde to achieve CH-PANI MGs using the inverse (water-in-oil) miniemulsion method. Interestingly, CH-PANI MGs exhibit polyampholyte behaviour and display charge-reversible behaviour (positive to negative charges) after treatment with a NaCl solution.
Results: The formed negatively charged N-CH-PANI MG aqueous solution is employed to load cationic vancomycin with a satisfactory loading efficiency of 91.3%, which is significantly higher than that of

---

Peer review under responsibility of Cairo University.

  * Corresponding authors at: Collaborative Innovation Center of Yangtze River Delta Region Green Pharmaceuticals, Zhejiang University of Technology, Hangzhou 310014, China (H. Li). College of Chemistry, Chemical Engineering and Biotechnology, Donghua University, Shanghai 201620, China (X. Shi). DWI-Leibniz-Institute for Interactive Materials e.V, 52056 Aachen, Germany (A. Pich).
    E-mail addresses: lihelin109280@zjut.edu.cn (H. Li), xshi@dhu.edu.cn (X. Shi), pich@dwi.rwth-aachen.de (A. Pich).

chitosan-based MGs. Moreover, N-CH-PANI MGs present lysozyme-triggered biodegradation and controllable vancomycin release upon the cleavage of glycosidic linkages of chitosan. In the simulated inflammatory intestinal microenvironment, vancomycin is rapidly released, and the cumulative release reaches approximately 76.9%. Remarkably, N-CH-PANI@VM MGs not only exhibit high resistance to harsh gastric acidity but also prevent the premature leakage of vancomycin in the healthy gastrointestinal tract. Encouragingly, the N-CH-PANI@VM MGs show obvious antibacterial activity against Staphylococcus aureus at a relatively low concentration of 20 μg/mL.

Conclusion: Compared to other pH-responsive carriers used to treat inflammatory bowel disease, the key advantage of lysozyme-responsive MGs is that they further specifically identify healthy and inflammatory intestines, achieving efficient inflammatory bowel disease treatment with few side effects. With this excellent performance, the developed smart MGs might be employed as a potential oral delivery system for inflammatory bowel disease treatment.

Introduction

Inflammatory bowel disease (IBD), a chronic inflammatory syndrome, is associated with many complications, e.g., bowel obstruction [1], chronic diarrhoea [2], rectal bleeding [3], and colorectal cancer [4]. Currently, more than 5 million people suffer from IBD worldwide, and the incidence rate increases annually, making IBD the third most common disease worldwide [5–7]. The conventional therapeutic strategy for IBD depends on antibiotics and immunosuppressive agents [8]. However, due to a lack of a targeted delivery capability and unsatisfactory bioavailability, the administration of high-dose agents is necessary to maintain an efficient drug concentration in the inflamed intestinal region, which will also lead to serious side effects and drug resistance [9–11]. Although direct rectal administration may provide an efficient drug concentration in targeted sites, this method is always accompanied by injury and severe pain [12,13]. Moreover, oral administration also increases drug efficacy and reduces side effects, but the drug always encounters the harsh acidic gastric environment, which alters stability and pharmaceutical effects [14,15]. Therefore, an intestinal inflammation-targeted drug delivery system must be developed that achieves gastric acid tolerance and controllable drug release to maximize the therapeutic efficacy and reduce side effects.

In recent years, smart microgels (MGs) have attracted increasing attention in the field of drug delivery due to their tunable particle size [16–18], excellent loading ability [19–21], and stimuli-responsive behaviour [22–24]. More importantly, MGs can be employed as a protective shell to enhance the tolerance of the loaded cargos to harsh environments [25–27]. Among them, chitosan (CH) has been approved by the FDA for biomedical applications because of its excellent biocompatibility [28–30]. Likewise, CH displays enzyme-triggered degradation, and some CH-based carriers have been developed for controlled and targeted drug release [31]. For instance, the integration of timolol maleate (TM)-loaded CH-based nanoparticles into contact lenses has been used to treat glaucoma [32]. The contact lens enables the controlled and sustained release of TM in the presence of lysozyme. Additionally, a novel wound-dressing biodevice incorporating epidermal growth factor (EGF) was designed using CH-based films, which are capable of slowly releasing EGF as required for normal wound repair [33]. Colombo *et al.* [34] constructed tamoxifen-loaded CH-based nanoparticles for lysozyme-triggered drug release in Caco-2 cells (a model of the intestinal epithelium). These results indicate that CH-based carriers show great promise in developing enzyme-triggered drug delivery systems. Moreover, as a unique cationic polysaccharide presents in nature, CH exhibits outstanding antibacterial and anti-inflammatory properties [35–37]. Notably, CH shows mucoadhesive properties by forming hydrogen bonds with mucins secreted from the intestinal epithe-

lium to obtain targeted intestinal delivery [38–40]. At present, pH-responsive MGs have been designed for controllable drug release in the intestinal region [41–43]. Nevertheless, some issues remain unsolved, such as the specific response to intestinal inflammation to achieve precise and controllable drug release [44]. In 2021, a review indicated that novel smart carriers not only facilitate targeted delivery but also should be able to respond to the infection site for sustained drug release, thereby enhancing the therapeutic effect and reducing potential adverse reactions [45].

Encouragingly, in a recent study, Bel *et al.* [46] found that intestinal pathogens disrupt cellular functions, thus resulting in abnormal secretion of lysozyme in the intestinal lumen against bacterial invasion. Depending on the inflammatory intestinal microenvironment, we designed vancomycin (VM)-loaded chitosan-polyaniline microgels (CH-PANI MGs) for the lysozyme-triggered release of VM. Aniline (ANI) was first grafted to CH to form CH-PANI polymers, which were crosslinked by glutaraldehyde (GA) to obtain CH-PANI MGs. Interestingly, CH-PANI MGs exhibit a charge-reversible behaviour (positive to negative charges) after treatment with a NaCl solution to form negatively charged N-CH-PANI MGs that are employed to load cationic vancomycin hydrochloride with a high loading efficiency. Moreover, N-CH-PANI MGs exhibit lysozyme-triggered biodegradation and controllable VM release upon the cleavage of glycosidic linkages of CH. In the simulated microenvironment of the inflamed intestine, VM is rapidly released from N-CH-PANI@VM MGs. Remarkably, N-CH-PANI@VM MGs not only exhibit high resistance to strong gastric acidity but also prevent the premature leakage of VM in the healthy gastrointestinal tract. The N-CH-PANI@VM MGs exhibit obvious antibacterial activity against *Staphylococcus aureus* (*S. aureus*). Based on this outstanding performance, the developed smart MGs with lysozyme-triggered VM release might be employed as a potential orally administered candidate for IBD treatment (Fig. 1).

Experimental

Synthesis of CH-PANI polymers and MGs

A series of CH-PANI copolymers with different ANI contents were prepared using oxidative polymerization (**Table S1**). Briefly, ANI (23.1–231.1 mg) dissolved in 1 M HCl (10 mL) and ammonium persulfate (APS) (28.1–281.0 mg) dissolved in 1 M HCl (2.5 mL) were added dropwise to a solution of 100 mg of CH dissolved in 0.1 M acetic acid (10 mL) with stirring at 0 °C in the dark for 1 h. Then, the solution was stirred at room temperature for another 5 h. After that, the solution was precipitated in ethanol (200 mL), and further purified by centrifugation, and washed with N-methylpyrrolidone (NMP) (3 times), ethanol (3 times), as well as
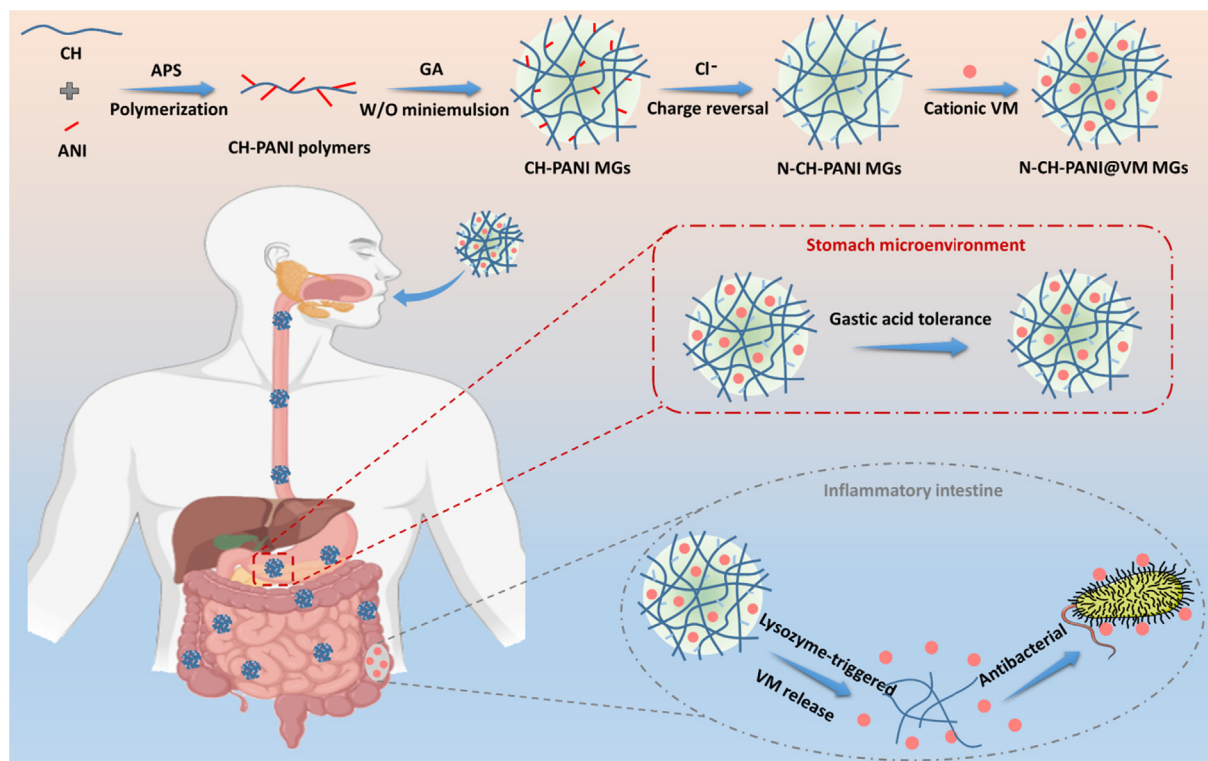
Fig. 1. Schematic preparation of charge-reversible and biodegradable CH-based MGs as potential oral delivery system for the IBD treatment by lysozyme-triggered antibiotics release: High VM loading, excellent acid tolerance, and specific inflammatory recognition.

water (3 times) respectively. Finally, the CH-PANI polymers were obtained by oven-dried (60 °C, 2 days).

CH-PANI MGs were prepared using an inverse miniemulsion method. Typically, CH-PANI polymers (10 mg) dissolved in 1 M HCl (1 mL) were mixed with GA (10 µL) as an aqueous phase, and Span 80 (258 mg) dissolved in cyclohexane (10 mL) as an organic phase. The mixture was ultrasonicated by a Misonix Sonicator (XL2000, Division of QSonica, LLC., Newtown, CT) at the duty cycle of 50% and output control of 40% in an ice bath for 10 min, and then stirred at room temperature for 16 h. Finally, the prepared CH-PANI MGs were purified by centrifugation (8000 rpm, 10 min), redispersed in water (10 mL) and transferred to a dialysis bag with molecular weight cut-off of 12–14 kDa for 3 days against water. Additionally, CH MGs were prepared as control samples under the same experimental conditions.

Synthesis of N-CH-PANI MGs and N-CH-PANI@VM MGs

The CH-PANI-2 MGs (1 mL) were treated with different concentrations of NaCl solution (1 mL) for 24 h to prepare charge-tunable MGs (**Table S3**). Among them, the CH-PANI-2 MGs treated with NaCl at a concentration ratio of 1:4 are termed N-CH-PANI MGs. Furthermore, the N-CH-PANI MGs were employed to load cationic VM. Typically, N-CH-PANI MGs (5 mg) and VM (1 mg) were immersed in 5 mL of water with stirring for 24 h in the dark. Afterwards, the N-CH-PANI@VM MGs were obtained by centrifugation to remove free VM (13000 rpm, 20 min). Additionally, CH@VM MGs and CH-PANI-2@VM MGs were prepared as control samples under the same experimental conditions.

In addition, the VM loading efficiency was measured by UV–vis spectroscopy at 280 nm depending on a calibration curve (**Fig. S1**) and estimated by equation (1):

$$VM\ loading\ efficiency = (M_o - M_n)/M_o \times 100\% \qquad (1)$$

where M_n and M_o represent the mass of the unloaded and the initial VM, respectively.

Lysozyme-triggered biodegradation and controllable VM release

The lysozyme-triggered degradation behaviour of N-CH-PANI MGs was investigated using dynamic light scattering (DLS) and transmission electron microscopy (TEM). The N-CH-PANI MGs (0.5 mg/mL) were dissolved in different media, namely, (a) pH 3.0 buffer, (b) pH 6.8 buffer, and (c) pH 6.8 buffer with lysozyme (50 µg/mL), and then TEM imaging along with a DLS analysis of NGs were conducted at predetermined time points (0–24 h). Among these media, pH 3.0 buffer was obtained by preparing acetate buffer (mixture of acetic acid and sodium acetate) as the simulated gastric fluid, pH 6.8 buffer was obtained by preparing phosphate buffered saline (PBS) as the simulated healthy intestine, and pH 6.8 buffer with lysozyme (50 µg/mL) was prepared as the simulated inflamed intestine.

The VM release kinetics of N-CH-PANI@VM MGs were evaluated in different simulated microenvironments. The N-CH-PANI@VM MGs (0.5 mg) in buffer solution (pH 3.0, 1 mL) were placed in a dialysis bag (MWCO = 50 kDa), suspended in buffer (pH 3.0, 9 mL) in the polyethylene tube, and incubated for 2 h. Next, the N-CH-PANI@VM MGs were changed to fresh buffer media (pH 6.8, 9 mL) with or without lysozyme (50 µg/mL) and incubated for 24 h. The release systems were placed in a vapour-bathed constant temperature vibrator at 37 °C. At each predetermined time interval, 1 mL of outer phase buffer from different systems was removed and the absorbance was measured at 280 nm using UV–vis spectroscopy; then, the same volume of the corresponding buffer was replenished. All release experiments of N-CH-PANI MGs as a control were repeated under each condition.

Cytocompatibility and antibacterial assay

Caco-2 cells were cultivated in Dulbecco's modified Eagle's minimal essential medium (DMEM, 25 mM glucose) supplemented with 10% (v/v) foetal bovine serum, 1% (v/v) nonessential amino acids, 1% (v/v) L-glutamine, and 1% (v/v) penicillin–streptomycin under 37 °C and 5% CO_2. A CCK-8 assay of Caco-2 cell viability was performed after the cells were treated with PBS or different concentrations of CH-PANI-2 MGs or N-CH-PANI MGs. Briefly, Caco-2 cells were first seeded in 96-well plates at a density of 5×10^3 cells per well with 200 μL of fresh medium and incubated for 24 h. Then, the medium in each well was replaced with fresh medium containing different final concentrations of CH-PANI-2 MGs or N-CH-PANI MGs (0.05–1 mg/mL) at pH 7.4. After 24 h of incubation, the medium was removed, and the cells were rinsed with PBS (3 times). Then, 200 μL of DMEM containing 10% CCK-8 reagent were added to each well, and the cells were incubated for 4 h in the dark. Finally, the cell viability was detected by measuring the absorbance at 450 nm via Multiskan MK3 ELISA reader (Thermo Scientific, Logan, UT).

Moreover, the antibacterial activity of each formulation was evaluated against *S. aureus*. Briefly, *S. aureus* was cultured in Mueller-Hinton broth at 37 °C for 12 h. The original *S. aureus* concentration was adjusted to 0.5 McFarland (10^6 CFU/mL) standard, and then bacteria were cultured in 96-well plates for the experiments. Then, the N-CH-PANI@VM MGs with or without lysozyme (50 μg/mL) were added to Mueller-Hinton broth (100 μL) at the final concentration ranging from 2.5 μg/mL to 50 μg/mL. Likewise, different concentrations of free lysozyme (2.5–50 μg/mL) were added to Mueller-Hinton broth. After 24 h of incubation, *S. aureus* viability was detected by measuring the absorbance at 630 nm *via* Multiskan MK3 ELISA reader (Thermo Scientific, Logan, UT). A blank sample with only Mueller Hinton Broth was used for the control.

Results and discussion

Synthesis and characterization of CH-PANI MGs

As mentioned above, CH exhibits a variety of excellent properties for treatment of patients with bowel diseases, such as good biocompatibility, enzyme-triggered degradation, and mucoadhesive behaviour. Moreover, conducting PANI exists as the emeraldine form or deprotonated (base) form above or below the isoelectric point, respectively. PANI may act as an anion or cation exchanger. Smart MGs composed of CH and PANI are expected to be biocompatible, and their charge-reversible properties can be used for efficient drug loading and controllable release in the inflamed intestinal region. First, a series of CH-PANI polymers with different ANI contents were prepared using oxidative polymerization using the method described in our previous study, with minor modifications (Fig. 2a) [47,48]. The detailed mechanism of oxidative polymerization is that the protonated ANI monomer is initiated by APS to form the intermediate of the PANI radical cation, while the hydrogen on the amino groups of CH is extracted by APS to form CH macro radicals, and then these two macroradicals recombine to obtain CH-PANI polymers (Fig. S2) [49]. The amounts of each component used for CH-PANI polymer preparation are listed in **Table S1**. In the FTIR spectra (Fig. 2b), the broad bands of the pure CH and CH-PANI polymers at 3200–3450 cm^{-1} are attributed to the stretching vibrations of the –NH_2 group. Compared to pure CH, the characteristic peaks at 1590 and 1502 cm^{-1} are related to the PANI part and attributed to C = C stretching vibrations in the quinoid and benzenoid rings, respectively, and the peak at 1154 cm^{-1} is attributed to the N = Q = N bending vibration (Q = quinonoid). Notably, the formed absorption peak at 747 cm^{-1} is derived from the –NH– group, indicating that the PANI has been grafted onto the CH skeleton. Furthermore, the content of ANI grafted onto CH-PANI polymers was quantitatively
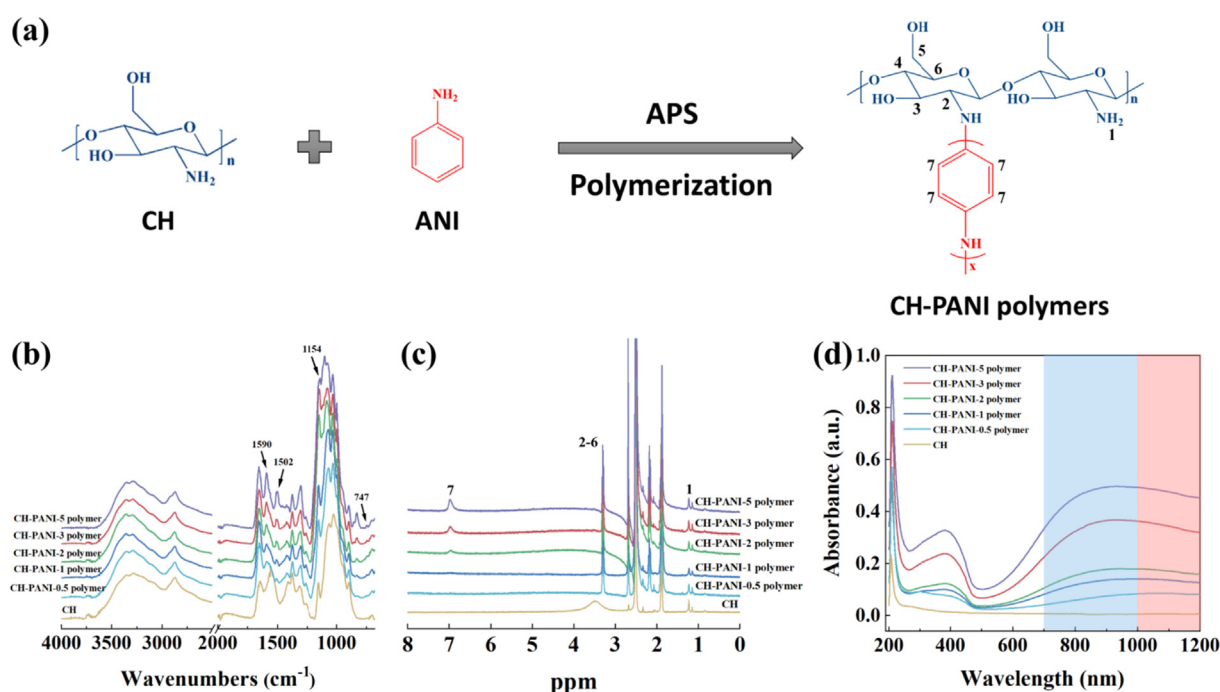

Fig. 2. (a) Schematic illustration of the synthesis of CH-PANI polymers. (b) FTIR, (c) ^{1}H NMR, and (c) UV–vis–NIR spectra of CH and CH-PANI polymers with different ANI contents.
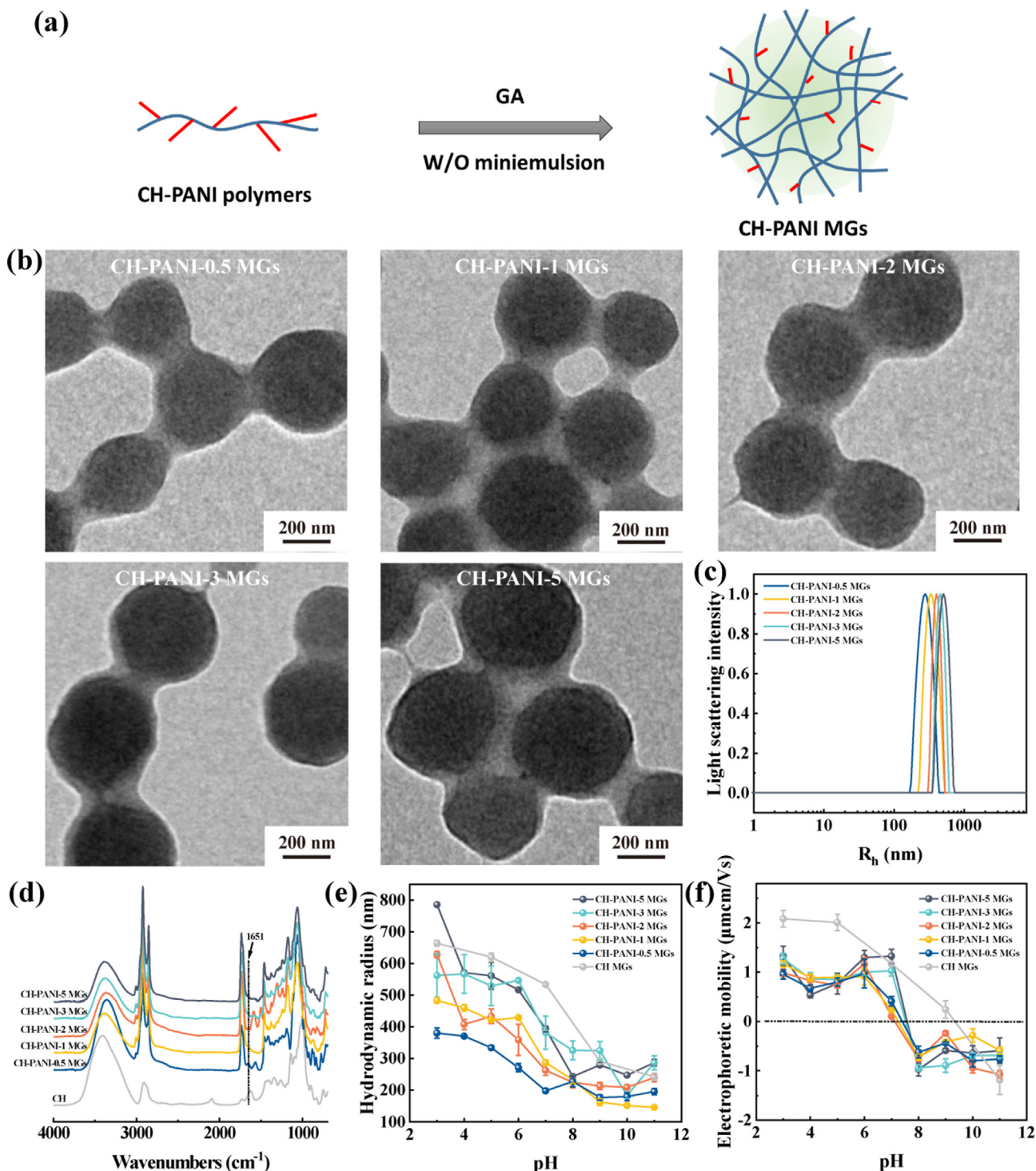
Fig. 3. (a) Schematic illustration of the synthesis of CH-PANI MGs. (b) TEM images of CH-PANI MGs with different ANI contents. (c) Hydrodynamic radius of CH-PANI MGs dispersed in water. (d) FTIR spectra of CH and CH-PANI MGs. (e) Hydrodynamic radius and (f) electrophoretic mobilities of CH-PANI MGs in buffers with different pH values.

analysed by recording ^{1}H NMR spectra (Fig. 2c). The new peak observed for CH-PANI polymers at approximately 7.0 ppm is related to the aromatic protons of PANI, and the peak intensity increases with the ANI content. Based on NMR integration, for CH-PANI-0.5 to CH-PANI-5 polymers, the ANI content was calculated to be 9.1, 13.8, 24.8, 37.9, and 48.7 mol%, respectively (**Table S1**). Likewise, in the UV–vis-NIR spectra (Fig. 2d), the CH-PANI polymers display a peak at 382 nm corresponding to the π–π* electron transition within the benzenoid segments and an obvi-

ous absorption in the NIR I and II regions (700–1200 nm) compared with that of pure CH. With the increase in the amount of grafted PANI, the absorption intensity of CH-PANI polymers increased.

Next, these CH-PANI polymers were crosslinked with GA to achieve the corresponding CH-PANI MGs *via* the inverse miniemulsion method (Fig. 3a). As shown in the TEM images, the CH-PANI MGs exhibit a uniform morphology and a radius of 186.2–219.8 nm in the dehydrated state (Fig. 3b). Furthermore, the hydrodynamic radius of CH-PANI MGs was determined to be

197.8–393.7 nm using DLS (Fig. 3c and Table S2). Notably, the size measured using DLS was larger than that measured from TEM images due to the swelling behaviour of CH-PANI MGs in aqueous solution. In the FTIR spectra (Fig. 3d), a new peak of CH-PANI MGs appearing at 1651 cm^{-1} is attributed to the Schiff base group (–N = CH–), suggesting that crosslinked bonds formed between the amino groups of polymers and aldehyde groups of GA [50].

Additionally, the pH-responsive behaviours of CH-PANI MGs were determined by performing DLS measurements (Fig. 3e). At different pH values (pH 3 to 11), the pure CH MGs displayed the maximum size shrinkage from 663.6 nm to 243.1 nm. In comparison, the CH-PANI MGs showed reduced shrinkage due to the lower number of amino groups. Furthermore, the electrophoretic mobilities of CH-PANI MGs were investigated (Fig. 3f). With increasing pH, the electrophoretic mobilities of CH MGs and CH-PANI MGs decreased and even reversed from positive to negative. In the acidic environment, the positive charge of MGs is contributed by the protonated amine groups. In the basic environment, the charge reversal of MGs is due to the formation of a Stern layer because the negatively charged counter ions overcompensate for the positive charge on the surface of MGs [51]. Notably, the charge reversal of CH-PANI MGs was easier to obtain under weakly alkaline conditions (pH 8) than pure CH MGs.

Adjustable charge and VM loading of N-CH-PANI MGs

To obtain the suitable nanocarriers for highly efficient loading of cationic antibiotics, it is essential to design the nanocarriers with adjustable charge. Based on the results described above, the CH-PANI MGs exhibit charge reversal properties under weakly alkaline

conditions. Moreover, our previous study revealed that the negative charge of MGs in aqueous solution is beneficial for the loading of cationic drugs [47]. Therefore, adjusting the charge of MGs in aqueous solution to a negative value at pH 7.0 is critical to increase the loading capacity of cationic antibiotics. In the next experiment, CH-PANI-2 MGs were chosen due to their lowest charge at pH 7.0. After treatment with NaCl at concentration ratios of 1:2 and 1:4, the charge of CH-PANI-2 MGs reversed from positive to negative at pH 7.0 (Fig. 4b and Table S3-S4). The specific attraction of negatively charged counteranions (Cl^{-}) by the PANI chains in the MGs allowed the formation of a negatively charged Stern layer, leading to an overcompensation for the positive charge on the surface of MGs (Fig. 4a) and thus reducing the electrophoretic mobility of MGs to negative values. These results are consistent with data reported in the previous literature [51–53]. The CH-PANI-2 MGs treated with NaCl solution at a concentration ratio of 1:4 (named N-CH-PANI MGs) showed an electrophoretic mobility of approximately −0.40 μmcm/Vs, indicating the good colloidal stability of N-CH-PANI MGs. In contrast, the CH MGs maintained a positive charge after treatment with NaCl solution.

Next, the loading efficiency of cationic VM in N-CH-PANI MGs in aqueous solution was investigated (Fig. 4c). The N-CH-PANI MGs exhibited the highest VM loading of 182.6 μg/mg at pH 7.0 due to the electrostatic interaction between negative N-CH-PANI MGs and cationic VM. Notably, the VM loading in CH MGs and CH-PANI-2 MGs was only approximately 36.4 and 69.4 μg/mg respectively, because of electrostatic repulsion. According to the calculation, the loading efficiency of N-CH-PANI@VM MGs was up to 91.3% and the values of CH@VM MGs and CH-PANI-3@VM MGs were 18.2% and 34.7%, respectively. Based on this result, the
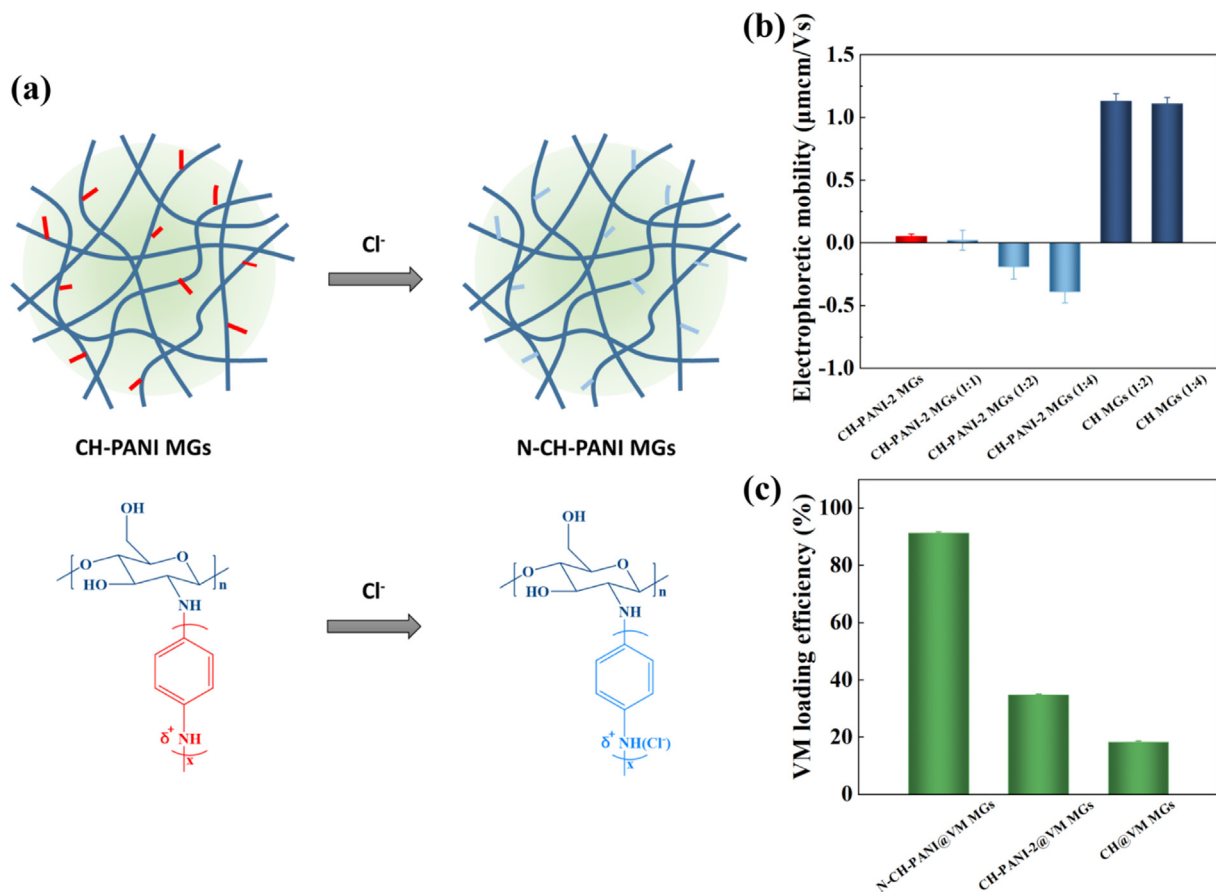

Fig. 4. (a) Schematic illustration of charge reversal of CH-PANI-2 MGs after treated with NaCl solution. (b) Electrophoretic mobilities of CH MGs and CH-PANI-2 MGs before and after treated with NaCl solution at different concentration ratios. (c) VM loading efficiency of N-CH-PANI@VM MGs, CH-PANI-2@VM MGs and CH@VM MGs.
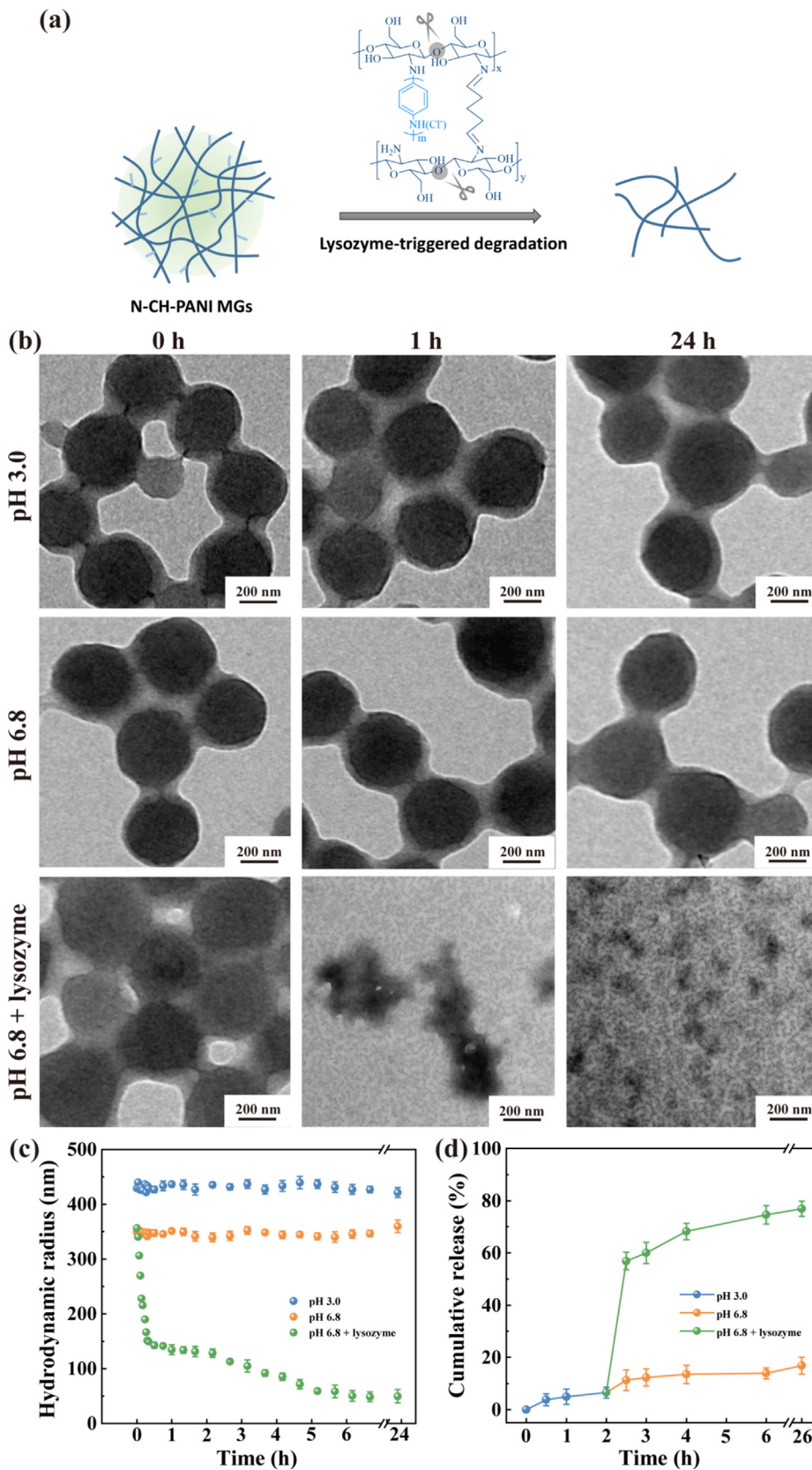
Fig. 5. (a) Schematic illustration of lysozyme-triggered biodegradation of N-CH-PANI MGs. (b) TEM images of N-CH-PANI MGs at different simulative microenvironments before and after degradation time for 24 h. (c) Hydrodynamic radius change of N-CH-PANI MGs at different simulative microenvironments over time. (d) Cumulative VM release profiles from N-CH-PANI@VM MGs at different simulative microenvironments.
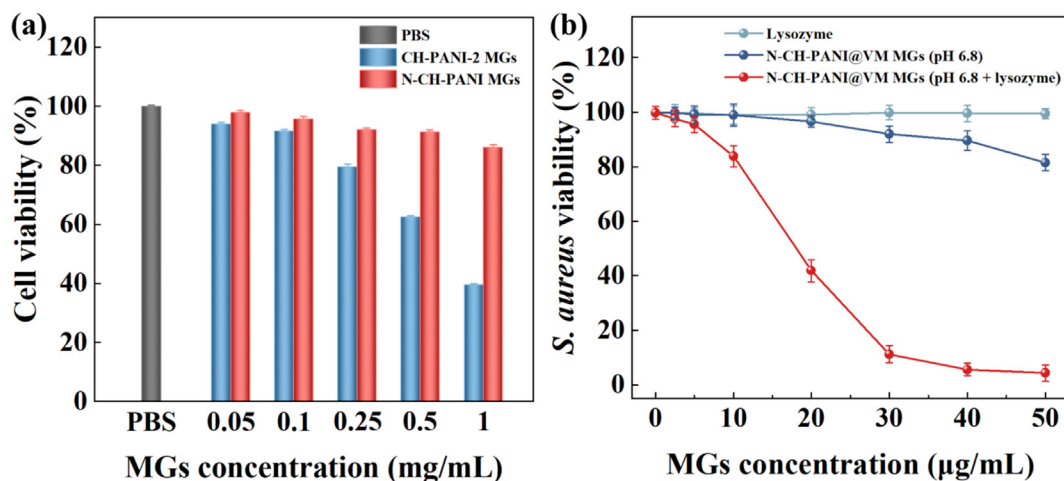
Fig. 6. (a) CCK-8 viability assay of Caco-2 cells treated with CH-PANI-2 MGs and N-CH-PANI MGs for 24 h, respectively. (b) Antibacterial effects of *S. aureus* treated with free lysozyme, N-CH-PANI@VM MGs (pH 6.8), and N-CH-PANI@VM MGs (pH 6.8 + lysozyme) for 12 h.

N-CH-PANI MGs, which are negatively charged carriers, are suitable for the highly efficient loading of cationic VM.

Lysozyme-triggered biodegradation and controlled VM release

For IBD treatments, the designed MGs should meet the requirements of precise release into the inflamed intestinal region and avoid premature drug leakage in the stomach or healthy intestine. In contrast to the stomach and healthy intestine, the inflamed intestine secretes a large amount of lysozyme to form a unique microenvironment [46]. Therefore, we explored the degradation of N-CH-PANI MGs in different simulated microenvironments. In the simulated gastric fluids (pH 3.0) or healthy intestine (pH 6.8), the morphology of N-CH-PANI MGs was intact after 24 h (Fig. 5**b**). In the inflammatory intestinal microenvironment (pH 6.8 + lysozyme), the N-CH-PANI MGs were completely decomposed. Furthermore, the change in the size of the N-CH-PANI MGs was monitored during one day to reveal the decomposition process (Fig. 5**c**). Clearly, in simulated gastric fluids (pH 3.0) or healthy intestines (pH 6.8), the size of the N-CH-PANI MGs remained unchanged. However, the size of the N-CH-PANI MGs rapidly decreased during the first 20 min, and then their size slowly decreased to approximately 50 nm within one day. The degradation mechanism is based on the enzymatic hydrolysis of the lysozyme-cleavable 1,4-β-glycosidic bonds in the CH backbone (Fig. 5**a**). Therefore, the N-CH-PANI MGs are capable of withstanding the harsh gastric acid microenvironment and then display lysozyme-triggered biodegradation in unique flamed intestinal areas.

Additionally, VM release from N-CH-PANI@VM MGs was determined by incubating the carrier in the simulated gastric fluids for 2 h and then incubating it in the simulated healthy or inflammatory intestinal microenvironment for 24 h to mimic gastrointestinal drug delivery by MGs after oral administration (Fig. 5**d**). Apparently, in the simulated gastric fluid (pH 3.0), the cumulative release of VM reached only approximately 6.5%. Upon the next test in the simulated healthy intestine (pH 6.8), VM was slowly released, and the cumulative release remained at approximately 16.8%. Notably, in the inflamed intestine (pH 6.8 + lysozyme), VM release was accelerated due to lysozyme-triggered degradation, especially in the first 30 min, and the final release rate reached 76.9%. Overall, these results reveal that the developed N-CH-PANI@VM MGs satisfy the oral administration requirements for IBD treatment, namely, excellent gastric acid tolerance, precise

release in the inflammatory intestine, and low leakage in the healthy gastrointestinal tract.

Biocompatibility and antibacterial effects

The biocompatibility of CH-PANI-2 MGs and N-CH-PANI MGs was evaluated by performing a CCK-8 assay of the viability of Caco-2 cells (Fig. 6**a**). After treatment with CH-PANI-2 MGs for 24 h, cell viability decreased with increasing concentrations of MGs, and the percentage of viable cells was only 39.6% when the concentration of MGs reached 1 mg/mL. Thus, the positively charged CH-PANI-2 MGs not only exhibit a low VM loading efficiency but also present high cytotoxicity due to the strong positive surface charge that destroys the integrity of negatively charged cell membranes. For comparison, the viability of cells treated with N-CH-PANI MGs was greater than 86.1%, even after treatment with the highest concentration of MGs (1 mg/mL), indicating that the N-CH-PANI MGs display satisfactory biocompatibility and may be employed as safe nanocarriers for biomedical applications.

The antibacterial effects of N-CH-PANI@VM MGs were examined against the gram-positive bacteria *S. aureus*, representing the bacterial model of IBD (Fig. 6**b**) [54,55]. In the control lysozyme group, the viability of *S. aureus* was maintained at a high level, indicating that lysozyme exerted almost no antibacterial effect at low concentrations (less than 50 μg/mL). Notably, in the N-CH-PANI@VM MG group (pH 6.8 + lysozyme), a concentration-dependent antibacterial effect was observed, and this treatment displayed obvious antibacterial activity at a relatively low MGs concentration of 20 μg/mL. In contrast, at the same concentration, much higher viability of *S. aureus* was observed in the group treated with N-CH-PANI@VM MGs (pH 6.8) in the absence of lysozyme. Based on these results, the N-CH-PANI@VM MGs exhibit lysozyme-triggered controllable VM release in response to intestinal inflammation, thus achieving a satisfactory therapeutic effect on IBD.

Conclusions

In summary, we developed smart carriers of VM-loaded CH-based MGs as potential oral delivery systems for IBD treatment. The prepared CH-PANI MGs exhibit polyampholyte behaviour and display a reversible charge after treatment with NaCl solution to form negatively charged N-CH-PANI MGs, which display a high loading efficiency of cationic VM by forming electrostatic interactions. Likewise, N-CH-PANI MGs exhibit lysozyme-triggered

biodegradation and controllable VM release. Remarkably, N-CH-PANI MGs provide a protective barrier for loaded VM against the harsh gastric environment, and prevent premature leakage of VM in the stomach. After oral administration, the carrier passes through the stomach to reach the intestine, and VM release from N-CH-PANI@VM MGs is specifically triggered by lysozyme in the inflamed intestinal region and avoids unnecessary release in the healthy intestine. The antibacterial experiments indicated that N-CH-PANI@VM MGs exhibit obvious antibacterial activity, even at a relatively low concentration. Compared with other pH-responsive carriers designed for IBD treatment, the key advantage of lysozyme-responsive MGs is that they further specifically identify healthy and inflamed intestines, achieving efficient IBD treatment with few side effects. This investigation provides information on a novel orally administered candidate for IBD treatment and increases attention to IBD-specific microenvironment-responsive carriers.

Compliance with Ethics Requirements

This article does not contain any studies with human or animal subjects.

CRediT authorship contribution statement

Xin Li: Conceptualization, Methodology, Software, Data curation, Writing – original draft. **Laura Hetjens:** Methodology, Software, Data curation. **Nadja Wolter:** Software, Data curation. **Helin Li:** Conceptualization, Methodology, Software, Data curation, Writing – original draft. **Xiangyang Shi:** Conceptualization, Supervision, Resources, Funding acquisition, Writing – review & editing. **Andrij Pich:** Conceptualization, Supervision, Resources, Funding acquisition, Project administration, Writing – review & editing.

Declaration of Competing Interest

The authors declare that they have no known competing financial interests or personal relationships that could have appeared to influence the work reported in this paper.

Acknowledgements

Appendix A. Supplementary material

Supplementary data to this article can be found online at https://doi.org/10.1016/j.jare.2022.02.014.

References

[1] Jaffe T, Thompson WM. Large-bowel obstruction in the adult: Classic radiographic and CT findings, etiology, and mimics. Radiology 2015;275(3):651–63.
[2] Farrell D, McCarthy G, Savage E. Self-reported symptom burden in individuals with inflammatory bowel disease. J Crohn's Colitisc 2016;10(3):315–22.
[3] Feagan BG, Lasch K, Lissoos T, Cao C, Wojtowicz AM, Khalid JM, et al. Rapid response to vedolizumab therapy in biologic-naive patients with inflammatory bowel diseases. Clin Gastroenterol Hepatol 2019;17(1):130–138.e7.
[4] Graham DB, Xavier RJ. Pathway paradigms revealed from the genetics of inflammatory bowel disease. Nature 2020;578(7796):527–39.
[5] Schirmer M, Garner A, Vlamakis H, Xavier RJ. Microbial genes and pathways in inflammatory bowel disease. Nat Rev Microbiol 2019;17(8):497–511.
[6] Chen F, Liu Q, Xiong Y, Xu L. Current strategies and potential prospects of nanomedicine-mediated therapy in inflammatory bowel disease. Int J Nanomed 2021;16:4225–37.
[7] Kaplan GG. The global burden of IBD: From 2015 to 2025. Nat Rev Gastroenterol Hepatol 2015;12(12):720–7.
[8] Vázquez-Baeza Y, Hyde ER, Suchodolski JS, Knight R. Dog and human inflammatory bowel disease rely on overlapping yet distinct dysbiosis networks. Nat Microbiol 2016;1:16177.
[9] Liu H, Cai Z, Wang F, Hong L, Deng L, Zhong J, et al. Colon-targeted adhesive hydrogel microsphere for regulation of gut immunity and flora. Adv Sci 2021;8(18):2101619. doi: https://doi.org/10.1002/advs.v8.1810.1002/advs.202101619.
[10] Zhang M, Viennois E, Prasad M, Zhang Y, Wang L, Zhang Z, et al. Edible ginger-derived nanoparticles: A novel therapeutic approach for the prevention and treatment of inflammatory bowel disease and colitis-associated cancer. Biomaterials 2016;101:321–40.
[11] Haider M, Zaki KZ, El Hamshary MR, Hussain Z, Orive G, Ibrahim HO. Polymeric nanocarriers: A promising tool for early diagnosis and efficient treatment of colorectal cancer. J Adv Res 2021. doi: https://doi.org/10.1016/j.jare.2021.11.008.
[12] Jiang J, Xiao J, Zhao Z, Yuan M-S, Wang J. One-step prepared nano-in-micro microcapsule delivery vehicle with sequential burst–sustained drug release for the targeted treatment of inflammatory bowel disease. Mater Chem Front 2021;5(16):6027–40.
[13] Lautenschläger C, Schmidt C, Fischer D, Stallmach A. Drug delivery strategies in the therapy of inflammatory bowel disease. Adv Drug Delivery Rev 2014;71:58–76.
[14] Zhang Q, Tao H, Lin Y, Hu Y, An H, Zhang D, et al. A superoxide dismutase/catalase mimetic nanomedicine for targeted therapy of inflammatory bowel disease. Biomaterials 2016;105:206–21.
[15] Wang Le, Yang J, Li S, Li Q, Liu S, Zheng W, et al. Oral administration of starting materials for *in vivo* synthesis of antibacterial gold nanoparticles for curing remote infections. Nano Lett 2021;21(2):1124–31.
[16] Li X, Sun H, Li H, Hu C, Luo Yu, Shi X, et al. Multi-responsive biodegradable cationic nanogels for highly efficient treatment of tumors. Adv Funct Mater 2021;31(26):2100227. doi: https://doi.org/10.1002/adfm.v31.2610.1002/adfm.202100227.
[17] Costa SA, Simon JR, Amiram M, Tang L, Zauscher S, Brustad EM, et al. Photo-crosslinkable unnatural amino acids enable facile synthesis of thermoresponsive nano- to microgels of intrinsically disordered polypeptides. Adv Mater 2018;30(5):1704878. doi: https://doi.org/10.1002/adma.v30.510.1002/adma.201704878.
[18] Li Y, Rodrigues J, Tomás H. Injectable and biodegradable hydrogels: Gelation, biodegradation and biomedical applications. Chem Soc Rev 2012;41(6):2193–221.
[19] Subbiah R, Hipfinger C, Tahayeri A, Athirasala A, Horsophonphong S, Thrivikraman G, *et al.* 3D printing of microgel-loaded modular microcages as instructive scaffolds for tissue engineering. *Adv Mater* 2020;**32**:2001736.
[20] Li X, Ouyang Z, Li H, Hu C, Saha P, Xing L, et al. Dendrimer-decorated nanogels: Efficient nanocarriers for biodistribution in vivo and chemotherapy of ovarian carcinoma. Bioact Mater 2021;6(10):3244–53.
[21] Li J, Guo M, Wang Y, Ye B, Chen Y, Yang X. Preparation of biological sustained-release nanocapsules and explore on algae-killing properties. J Adv Res 2021;31:87–96.
[22] Xu W, Rudov A, Oppermann A, Wypysek S, Kather M, Schroeder R, et al. Synthesis of polyampholyte Janus-like microgels by coacervation of reactive precursors in precipitation polymerization. Angew Chem Int Ed 2020;59(3):1248–55.
[23] Li X, Lu S, Xiong Z, Hu Y, Ma D, Lou W, et al. Light-addressable nanoclusters of ultrasmall iron oxide nanoparticles for enhanced and dynamic magnetic resonance imaging of arthritis. Adv Sci 2019;6(19):1901800.
[24] Sun M, He Le, Fan Z, Tang R, Du J. Effective treatment of drug-resistant lung cancer via a nanogel capable of reactivating cisplatin and enhancing early apoptosis. Biomaterials 2020;257:120252. doi: https://doi.org/10.1016/j.biomaterials.2020.120252.
[25] Zhu M, Wei K, Lin S, Chen X, Wu C-C, Li G, et al. Bioadhesive polymersome for localized and sustained drug delivery at pathological sites with harsh enzymatic and fluidic environment via supramolecular host-guest complexation. Small 2018;14(7):1702288.
[26] Shrestha N, Shahbazi M-A, Araújo F, Mäkilä E, Raula J, Kauppinen EI, et al. Multistage pH-responsive mucoadhesive nanocarriers prepared by aerosol flow reactor technology: A controlled dual protein-drug delivery system. Biomaterials 2015;68:9–20.
[27] Li X, Kong L, Hu W, Zhang C, Pich A, Shi X, et al. Safe and efficient 2D molybdenum disulfide platform for cooperative imaging-guided photothermal-selective chemotherapy: A preclinical study. J Adv Res 2021. doi: https://doi.org/10.1016/j.jare.2021.08.004.
[28] Kumar AM, Suresh B, Das S, Obot IB, Adesina AY, Ramakrishna S. Promising bio-composites of polypyrrole and chitosan: Surface protective and in vitro biocompatibility performance on 316L SS implants. Carbohydr Polym 2017;173:121–30.
[29] Feng X, Du C, Li J. Molecular assembly of polysaccharide-based microcapsules and their biomedical applications. Chem Rec 2016;16(4):1991–2004.

[30] Li X, Yue X, Wang J, Liang X, Jing L, Lin Li, et al. Prussian blue nanoparticle-loaded microbubbles for photothermally enhanced gene delivery through ultrasound-targeted microbubble destruction. Sci Bull 2016;61(2):148–56.

[31] Åhlén M, Tummala GK, Mihranyan A. Nanoparticle-loaded hydrogels as a pathway for enzyme-triggered drug release in ophthalmic applications. Int J Pharm 2018;536(1):73–81.

[32] Kim H-J, Zhang K, Moore L, Ho D. Diamond nanogel-embedded contact lenses mediate lysozyme-dependent therapeutic release. ACS Nano 2014;8 (3):2998–3005.

[33] Picheth GF, Sierakowski MR, Woehl MA, Ono L, Cofré AR, Vanin LP, et al. Lysozyme-triggered epidermal growth factor release from bacterial cellulose membranes controlled by smart nanostructured films. J Pharm Sci 2014;103 (12):3958–65.

[34] Barbieri S, Sonvico F, Como C, Colombo G, Zani F, Buttini F, et al. Lecithin/chitosan controlled release nanopreparations of tamoxifen citrate: Loading, enzyme-trigger release and cell uptake. J Controlled Release 2013;167(3):276–83.

[35] Su Lu, Feng Y, Wei K, Xu X, Liu R, Chen G. Carbohydrate-based macromolecular biomaterials. Chem Rev 2021;121(18):10950–1029.

[36] Sahariah P, Másson M. Antimicrobial chitosan and chitosan derivatives: A review of the structure–activity relationship. Biomacromolecules 2017;18 (11):3846–68.

[37] Zheng K, Tong Yu, Zhang S, He R, Xiao L, Iqbal Z, et al. Flexible bicolorimetric polyacrylamide/chitosan hydrogels for smart real-time monitoring and promotion of wound healing. Adv Funct Mater 2021;31(34):2102599.

[38] Yang C, Merlin D. Nanoparticle-mediated drug delivery systems for the treatment of IBD: Current perspectives. Int J Nanomed 2019;14:8875–89.

[39] Mumuni MA, Kenechukwu FC, Ofokansi KC, Attama AA, Díaz DD. Insulin-loaded mucoadhesive nanoparticles based on mucin-chitosan complexes for oral delivery and diabetes treatment. Carbohydr Polym 2020;229:115506. doi: https://doi.org/10.1016/j.carbpol.2019.115506.

[40] Sogias IA, Williams AC, Khutoryanskiy VV. Why is chitosan mucoadhesive? Biomacromolecules 2008;9(7):1837–42.

[41] Huang Z, Gan J, Jia L, Guo G, Wang C, Zang Y, et al. An orally administrated nucleotide-delivery vehicle targeting colonic macrophages for the treatment of inflammatory bowel disease. Biomaterials 2015;48:26–36.

[42] Ali H, Weigmann B, Neurath MF, Collnot EM, Windbergs M, Lehr C-M. Budesonide loaded nanoparticles with pH-sensitive coating for improved mucosal targeting in mouse models of inflammatory bowel diseases. J Controlled Release 2014;183:167–77.

[43] Karban A, Nakhleh MK, Cancilla JC, Vishinkin R, Rainis T, Koifman E, et al. Programmed nanoparticles for tailoring the detection of inflammatory bowel diseases and irritable bowel syndrome disease via breathprint. Adv Healthcare Mater 2016;5(18):2339–44.

[44] Zhang S, Langer R, Traverso G. Nanoparticulate drug delivery systems targeting inflammation for treatment of inflammatory bowel disease. Nano Today 2017;16:82–96.

[45] Kalelkar PP, Riddick M, García AJ. Biomaterial-based antimicrobial therapies for the treatment of bacterial infections. Nat Rev Mater 2022;7(1):39–54.

[46] Bel S, Pendse M, Wang Y, Li Y, Ruhn KA, Hassell B, et al. Paneth cells secrete lysozyme via secretory autophagy during bacterial infection of the intestine. Science 2017;357(6355):1047–52.

[47] Li X, Li H, Zhang C, Pich A, Xing L, Shi X. Intelligent nanogels with self-adaptive responsiveness for improved tumor drug delivery and augmented chemotherapy. Bioact Mater 2021;6(10):3473–84.

[48] Li H, Li X, Jain P, Peng H, Rahimi K, Singh S, et al. Dual-degradable biohybrid microgels by direct cross-linking of chitosan and dextran using azide–alkyne cycloaddition. Biomacromolecules 2020;21(12):4933–44.

[49] Tiwari A, Shukla SK. Chitosan-g-polyaniline: A creatine amidinohydrolase immobilization matrix for creatine biosensor. Express Polym Lett 2009;3 (9):553–9.

[50] Guo B, Finne-Wistrand A, Albertsson A-C. Facile synthesis of degradable and electrically conductive polysaccharide hydrogels. Biomacromolecules 2011;12 (7):2601–9.

[51] Cabuk M, Yavuz M, Unal HI. Electrokinetic properties of biodegradable conducting polyaniline-graft-chitosan copolymer in aqueous and non-aqueous media. Colloids Surf, A 2014;460:494–501.

[52] Asturias GE, Jang G-W, Macdiarmid AG, Doblhofer K, Zhong C. Membrane-properties of polymer-films: The acid-doping reaction of polyaniline. Ber Bunsen-Ges Phys Chem 1991;95(11):1381–4.

[53] Çabuk M. Colloidal behaviors of conducting polymer/chitosan composite particles. In: Rahman MM, Asiri AM, editors. Advances in colloid science. London: IntechOpen; 2016. p. 177–88.

[54] Azimirad M, Krutova M, Balaii H, Kodori M, Shahrokh S, Azizi O, et al. Coexistence of Clostridioides difficile and Staphylococcus aureus in gut of Iranian outpatients with underlying inflammatory bowel disease. Anaerobe 2020;61:102113. doi: https://doi.org/10.1016/j.anaerobe.2019.102113.

[55] Cong Y, Yang S, Rao X. Vancomycin resistant Staphylococcus aureus infections: A review of case updating and clinical features. J Adv Res 2020;21:169–76.